

Neuromodulatory control over nonlinear spiking of layer V pyramidal neurons mediates adaptive slightly subcritical network dynamics

Authors: Brandon R. Munn^{1,2,*}, Eli J. Müller^{1,2}, and James M. Shine¹.

Affiliations

¹ Brain and Mind Centre, The University of Sydney, Sydney, New South Wales, Australia

² Complex Systems, School of Physics, The University of Sydney, Sydney, New South Wales, Australia.

* Correspondence to: brandon.munn@sydney.edu.au.

Abstract

To remain adaptable to a dynamic environment, coordinated neural activity in the brain must be simultaneously flexible and reliable. There is evidence that the brain facilitates this adaptive response using highly-conserved metabotropic neuromodulatory neurotransmitters, such as noradrenaline and acetylcholine. While we understand how these neuromodulators alter individual neuronal dynamics, precisely how neuromodulation operates in networks of neurons to give rise to observed large-scale dynamics remains unknown. By viewing neural dynamics as a critical phase transition, neuromodulators can be framed as control parameters that modulate the order inherent within a network of linear neurons – analogous to magnetic domains in the Ising model. While powerful, this view fails to account for two significant biological aspects: distinct arms of the neuromodulatory system possess differential anatomical projection patterns; and, neurons are not simple linear point sources. Neurons can spike nonlinearly, whereby the same input can elicit different responses. Here, we investigate this disparity by demonstrating correspondence between adaptive information processing modes – calculated on *in vivo* electrophysiological recordings of bursting layer V neurons in awake mice – and fluctuations in neuromodulatory tone – assessed by dynamic changes in pupil diameter. We theoretically validate these results by creating a novel, biologically plausible dual-compartment model of nonlinear layer V pyramidal neurons – capable of both regular spike and bursting modes – that reproduce our main empirical findings. We then probe our model at a resolution impossible *in vivo* to demonstrate that the adrenergic and cholinergic neuromodulatory systems shift the brain into a neuroprotective (i.e., slightly subcritical) regime – assessed by the branching parameter – while facilitating flexible and reliable dynamics, respectively. This unexpected result demonstrates that the brain has circumvented the necessity to shift the system closer to criticality for variability by differentially augmenting an intrinsic neuronal nonlinearity. Our analyses establish that these distinct arms of the ascending arousal system modulate ensembles of layer V pyramidal neurons to augment critical dynamics and facilitate distinct adaptive information processing modes within the brain.

Introduction

How to successfully overcome an uncertain, unconstrained, and dynamic situation – be that through continuing with the current strategy (reliability), switching strategies (flexibility), or assessing alternative strategies (sensitivity) – is a fundamental problem faced by all living organisms. How the brain supports these different information processing modes while retaining the ability to respond with a high degree of specificity to distinct ethological contexts remains an important open question in neuroscience. By altering the excitability and receptivity of targeted neurons distributed through the brain [1], the ascending neuromodulatory system is well-placed to solve this dilemma. The neuromodulatory system allows the brain to separate the control of the information processing modes of the brain from the processing of specific bits of information. In this way, the brain can flexibly and adaptively transition between distinct neural states that arise from dynamic endogenously and exogenously driven demands in a manner that does not infringe upon the ongoing information processing strategies.

While there are many unique arms of the ascending arousal system [1], the concentration (Fig. 1A) of two highly-conserved metabotropic neurotransmitters – noradrenaline (NAd) and acetylcholine (ACh) – has been argued to transition the brain into distinct states with unique computational benefits [2]. For instance, fluctuating levels of NAd in the cerebral cortex have been associated with striking an optimal balance between exploratory and exploitative behaviour [3], whereas ACh levels are typically associated with states of focussed attention [4]. Recent studies have demonstrated how these neuromodulators alter individual neuronal activity [5,6]; nonetheless, how neuromodulation operates in networks of neurons to give rise to the observed emergent nonlinear dynamics remains poorly understood.

Concepts from physics are well suited for understanding the collective phenomena of the brain [1]. In particular, the critical brain hypothesis

has been thoroughly investigated [7–9]. Briefly, this hypothesis posits that the brain is poised near the critical point [7], as these regimes are endowed with numerous beneficial properties, such as the ability to strike an optimal balance between flexibility and reliability, as well as the capacity to operate across broad spatiotemporal scales [9–11] and optimize information transfer between itself and the complex natural environment [9,12–14]. Using this approach the collective dynamics of a system can be effectively described by order parameters that are altered by control parameters – for instance, in the well-known Ising model, magnetism is an order parameter that is altered by a control parameter of temperature [15]. To the extent that the brain exhibits features of criticality, as it appears that it does [9,16,17], we can then ask what features of the brain may act as control parameters.

In previous work, we have argued that the neuromodulatory arousal system is well-placed to act as a control parameter in the brain [1,2,18,19]. The arousal system is comprised of a set of neurons in the brainstem and forebrain that send a diverse set of axonal projections to the rest of the central nervous system in unique ways that suggest unique functional consequences [2]. For instance, due to diffuse projections of the locus coeruleus (Fig.1A red), NAd is hypothesized to act as a global control parameter – like temperature in the Ising model. In contrast, the brain can simultaneously different control parameters beyond this one-dimensional case, as cortical projections from the basal nucleus of Meynert project in a much more targeted fashion (Fig.1A blue), suggesting that ACh acts as a spatially localized control parameter preferentially altering local coordination.

The site of action of neuromodulation is also of crucial importance. Previous theories of neural criticality have treated individual neurons as linear point processes [12,16,20]. However, many neurons in the cerebral cortex are nonlinear – the same input can elicit different responses – suggesting that the neuromodulatory system could, in principle, confer

even more powerful computational benefits on the brain than have been previously appreciated. The paradigmatic example of a nonlinear neuron is the thick-tufted Layer V pyramidal neurons (LV_{PN}), the principal output neuron of the cerebral cortex and capable of dual spiking modes [21–23]. LV_{PN} possess two dendritic compartments – somatic and apical – that are electrotonically separated at rest by hyperpolarisation-activated cyclic nucleotide-gated (HCN) channels located along the dendritic apical trunk (Fig. 1B). This separation ensures that inputs to the apical dendrites do not typically affect spiking dynamics in the soma, which are instead driven solely by inputs close to the soma [24,25]. When the dendritic compartments are coupled – e.g., via closure of HCN channels or non-specific thalamic drive – calcium spikes in the apical layer can propagate down the apical trunk allowing high-frequency burst firing (Fig. 1C; [23]), during which somatic sodium spikes ride atop the slower calcium spike [6]. In this way, LV_{PN} spiking dynamics are nonlinearly dependent upon the state of the cell and the broader network [26].

Recent studies have confirmed that integral functions of the brain – such as conscious awareness and binding feedforward and feedback signals [6,22] – are coordinated through LV_{PN} bursting. Significantly, this bursting is modulated by adrenergic and cholinergic neuromodulation [5,6,27], suggesting that neuromodulatory control over LV_{PN} may be responsible for many computational benefits that this nonlinear mechanism might confer to the brain. Based on this work [5,6,27] and our previous theoretical predictions [2], we hypothesize that ACh and NAd act as orthogonal control parameters for systems-level neuronal dynamics through the modulation of voltage-gated ion channels [1] on the apical dendrites of LV_{PN} [27]. In the remainder of this manuscript, we provide both empirical and computational evidence that confirms these predictions.

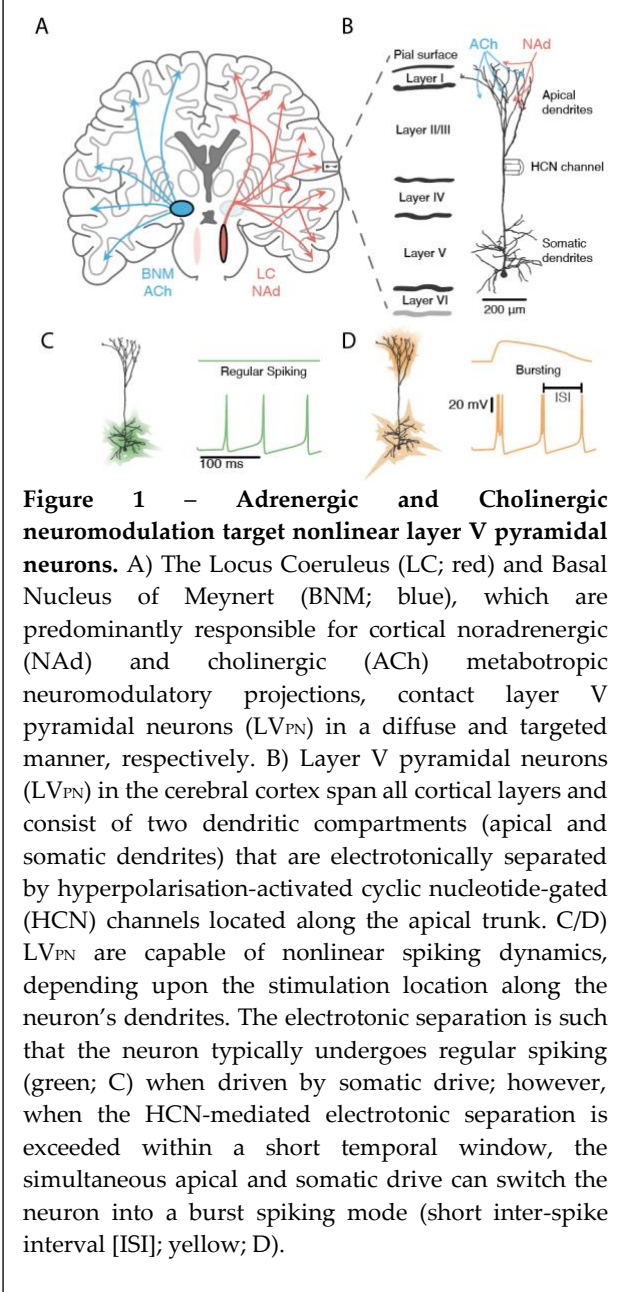
Results:

Electrophysiological Evidence for

Neuromodulatory Mediated Signatures of Criticality

As a first step, we sought first to confirm evidence of criticality in LV_{PN} . To this end, we re-analyzed *in vivo* spontaneous electrophysiological neural activity recorded from three awake mice (*Mus musculus*) [28] collected from eight invasive silicon neuropixels probes (Fig. 2A) in combination with pupil recordings (Fig. 2B) [29]. These recordings provide high-resolution access to multiple cortical neurons in awake animals. To isolate bursting neurons in Layer V, we applied two different criteria: first, we selectively analyzed neuronal units that were identified on channels referenced to Layer V of the Allen Mouse Common Coordinate Framework [30]; and second, we also identified units that demonstrated a bimodal ISI distribution, defined as satisfying $b_{ISI}/n_{ISI} > 10\%$, where b_{ISI} is the number of $ISI < 10\text{ms}$ and n_{ISI} is the total number of ISI. This approach ensured that we identified cells within Layer V that demonstrated both bursting (i.e., short ISI) and ‘regular’ spiking (i.e., long ISI) modes; (Fig. 2C). This procedure identified 148 Layer V bursting units across eight visual and motor sensory regions. To support this claim, we further confirmed that the mean burst ratio of the isolated units ($\beta_{mouse} = \frac{b_{ISI}}{n_{ISI}} = 0.26 \pm 0.13 \text{ s.d.}$) was consistent with observed bursting ratios of LV_{PN} [23].

To test our hypothesis, we also required a continuous measure of neuromodulatory tone, which is challenging to measure directly in the brain *in vivo* without techniques like microdialysis (which was not available in this dataset) [31]. Despite this limitation, we were able to utilize fluctuations in pupil diameter as an indirect measure of neuromodulatory tone: the pupil dilates with increases in adrenergic tone (Fig. 2B; left, red) and constricts with increases in cholinergic tone (Fig. 2B; left, blue) [31,32]. Based on consternation in the literature, we re-analyzed the relationship between cortical NAd and ACh tone and pupil diameter in mice (see Supp.S1 for further details) [31]. Figure. 2B demonstrates that rapid fluctuations in pupil diameter, p_d , (i.e., dp_d/dt ; Fig.



2B right) are strongly related to the balance between systemic adrenergic and cholinergic tone in the cerebral cortex, and hence can be used as an indirect readout of neuromodulatory tone in the brain.

With these estimates of LV_{PN} burst-firing and neuromodulatory tone in place, we next required a means for evaluating evidence of criticality. Typically, we would quantify this as the proximity to the critical point; however, due to the non-stationarity of neuromodulatory tone, we cannot infer this directly from the dynamics [33]. Nevertheless, we can calculate signatures of

criticality in the empirical recordings, particularly via the increase in variability of the order parameter at the critical point - due to the divergence of the order parameters derivative [15]. To measure these properties in spiking data, we first calculated two distinct and commonly utilized neural order parameters: the population spike count,

$$\rho_t = \frac{1}{N} \sum_i \delta(t - t_i), \quad (1)$$

which represents the number of spikes at time t_i across N neurons [34] and the mean temporal coherence between neuronal spiking activity,

$$\theta_t = \frac{1}{N} \sum_{j=1}^N |e^{i\phi_{tj}}|, \quad (2)$$

where ϕ_t is the phase of the spike count obtained via the Hilbert transform [20], and then we calculated the susceptibility as,

$$\chi = \langle \rho_t^2 \rangle - \langle \rho_t \rangle^2, \quad (3)$$

where $\langle \dots \rangle$ represents the mean, quantifying the variability of the population spiking dynamics (Fig. 2D blue) [9,35]. We also calculated the transient coherence as,

$$\Psi = \langle \theta_t^2 \rangle - \langle \theta_t \rangle^2, \quad (4)$$

quantifying the variability in the coordinated spiking phase (Fig. 2D yellow) [10,11]. Both measures track the spatiotemporal variance of order parameters of the system - in this way, the diversity of spatiotemporal spiking coordination can be summarized to indicate the available information bandwidth of the system. For instance, large χ and Ψ suggests an extensive repertoire of utilized neuronal assemblies, which indicates a responsive and flexible information processing mode [20]. In contrast, small χ and Ψ indicate that variability is quenched into a precise bandwidth, indicating a reliable information processing mode [11,36].

Using this approach, we set out to test the hypothesis that NAd and ACh differentially affect systems-level information processing dynamics [31]. We predicted that fluctuations in pupil diameter, dp_d/dt , should differentiate distinct signatures of systems-level neural dynamics: phasic increases in NAd (i.e., pupil dilation; increased dp_d/dt) should precede heightened χ and Ψ , whereas phasic increases in ACh (i.e., pupil constriction; decreased dp_d/dt) should precede decreases in both χ and Ψ . To assess these dynamic changes in both χ and Ψ with fluctuations in pupil diameter, we utilized time-varying estimates:

$$\hat{\chi} = \left| \frac{d\rho}{dt} \right|, \quad (5)$$

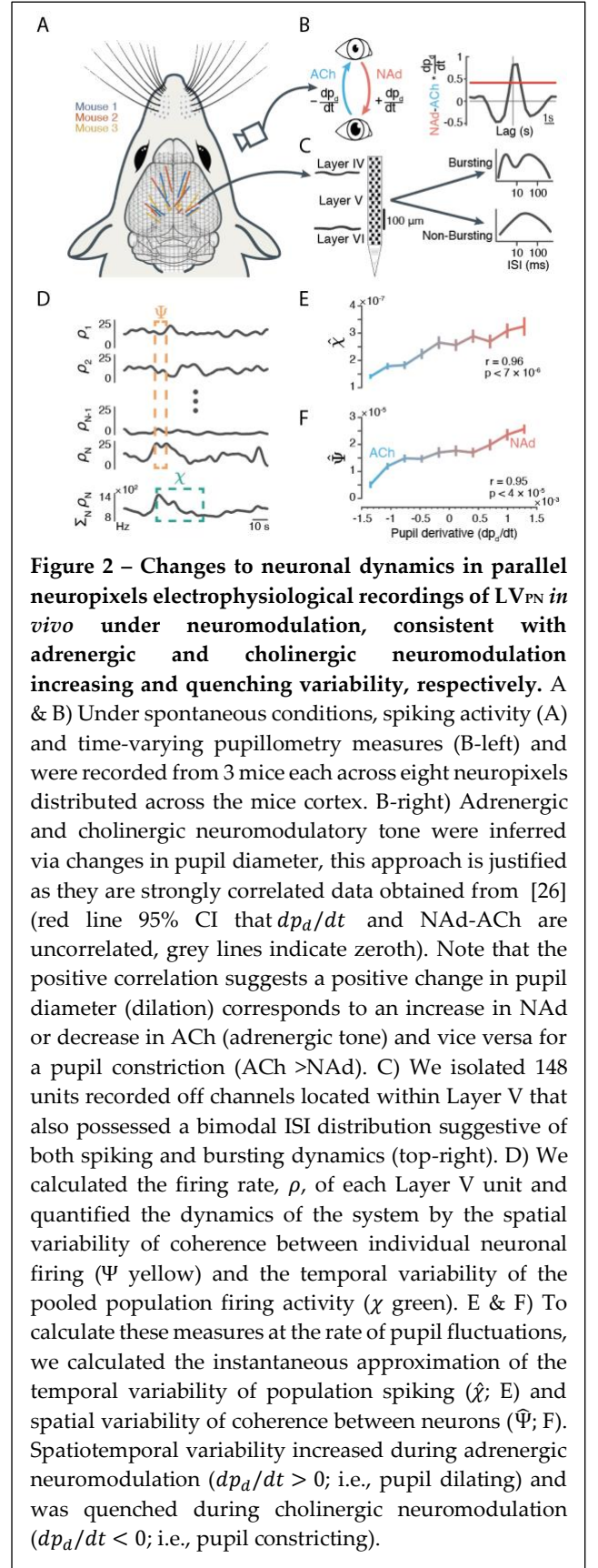
$$\hat{\Psi} = \left| \frac{d\theta}{dt} \right|, \quad (6)$$

respectively. Our analysis confirmed our hypothesis: specifically, we observed robust positive (negative) relationships between pupillary dilation (constriction; Fig. 2B) and both $\hat{\chi}$ ($p < 7 \times 10^{-6}$; Fig. 2E) and $\hat{\Psi}$ ($p < 4 \times 10^{-5}$; Fig. 2F).

Theories of neuromodulation hold that adrenergic and cholinergic can shift the neuronal system between flexible dynamics, in which neuronal spiking is highly variable in both space and time, and reliable dynamics, in which neuronal spiking patterns are more spatiotemporally constrained [31]. Our results confirm that an increase in NAd (ACh) tone leads to the enhancing (quenching) of the spiking variability and coherence of LV_{PN} in recordings from an awake, freely behaving mouse *in vivo*. In this way, our results demonstrate a direct relationship between adrenergic neuromodulation and flexible dynamics and cholinergic neuromodulation and reliable dynamics at the network scale.

We found that adrenergic and cholinergic mediate signatures of criticality; however, we wondered whether this was due to either changing the system's proximity to the critical point or emerging from a

nonlinear dynamic of the LV_{PN} dual compartments – or a combination of both. Nonetheless, the dynamic



nature of neuromodulation during *in vivo* recordings and the difficulty from recording from both apical and somatic compartments. Thus, to answer this question, we required a biologically plausible model of LV_{PN} – with apical and somatic compartments – able to reproduce the dual spiking dynamics.

A Biologically Plausible Network Model of Nonlinear Layer V Pyramidal Neurons Recapitulates Adaptive Dynamics Under Neuromodulation

To discern the mechanistic origin of this critical phenomenon, we constructed a biologically plausible, spatially embedded neuronal network (Fig. 3A), in which model neurons consisted of two compartments designed to mimic the dual compartment coupling of LV_{PN} [24]. The somatic compartment was modelled as an Izhikevich neuron [37] given by two coupled ODEs

$$\frac{dv}{dt} = 0.04v^2 + 5v - u + I, \quad (7)$$

$$\frac{du}{dt} = a(b(v - v_r) - u), \quad (8)$$

where v represents the membrane potential (mV), I represents all current into the neuron, $a = 0.02 \text{ ms}^{-1}$ represents the time constant of the spike adaptation current, $b = 0.2 \text{ nS}$ describes the sensitivity of the adaptation current to subthreshold fluctuations of the membrane potential, and v_r represents the reset voltage, where the spike reset is

$$\text{if } v \geq 30, \text{ then } \begin{cases} v \leftarrow c(t) \\ u \leftarrow u + d(t) \end{cases}. \quad (9)$$

The somatic compartment is coupled to an apical compartment that acted as a temporal integrator switch. The presence of coincident apical drive that exceeded the apical-somatic electrotonic separation within a 30ms window [38] caused the apical compartment to switch the somatic spiking properties from empirically observed LV_{PN} regular spiking ($c(t) = -65, d(t) = 8$) to a burst firing behaviour ($c(t) = -55, d(t) = 4$; see Supp.S2 for full-details) [39]. The somatic compartments were

coupled to one another via biophysical difference-of-Gaussian (i.e., ‘Mexican-hat’) synaptic coupling weight w_{ij} ,

$$w_{ij} = \begin{cases} 0 & \text{if } d_{ij} > d_{max} \text{ or } i = j \\ C_E e^{-\frac{d_{ij}^2}{d_E}} + C_I e^{-\frac{d_{ij}^2}{d_I}} & \text{if } 0 < d_{ij} < d_{max} \end{cases}, \quad (10)$$

where d_{ij} is the Euclidean distance between neuron i and j , C_E and C_I are the excitatory and inhibitory coupling constants, and d_E and d_I are the excitatory and inhibitory coupling ranges. This coupling has been demonstrated to capture both local excitatory and inhibitory effects of LV_{PN} [40]. Results presented are for $N^2 = 4,900$ neurons (a 70×70 grid) simulated for $T = 20\text{s}$ at a temporal resolution of $dt = 0.5\text{ms}$, and results were consistent for grid sizes $N = 50$ to 200 and $T = 5$ to 50s (see Supplementary for a detailed description).

Typical neuronal modelling focuses on either the single neuron – at a multi-compartment resolution – or a network of neurons – each at a point-neuron resolution. By utilizing our novel dual-compartment Izhikevich network model, we were able to create biologically plausible spike profiles while retaining computational efficiencies (i.e., avoiding multiple channel kinetics across multiple compartments) [23]. In this way, we were able to examine the network-level interactions of ensembles of thousands of LV_{PN} under a precise combination of neuromodulatory control that would be impossible *in vivo*.

To systematically examine the effect of neuromodulation on LV_{PN} dynamics, we simplified our model parameter space to investigate two independent parameters influenced by neuromodulation. Specifically, we investigated the probability that apical drive exceeds the apical-somatic HCN electrotonic separation leading to bursting, β (Fig. 3B). This parameter captures any effects that alter either HCN channel properties or the excitability of apical dendrites. β ranges from $\beta = 0$ where LV_{PN} cells cannot burst to $\beta = 1$ where LV_{PN}

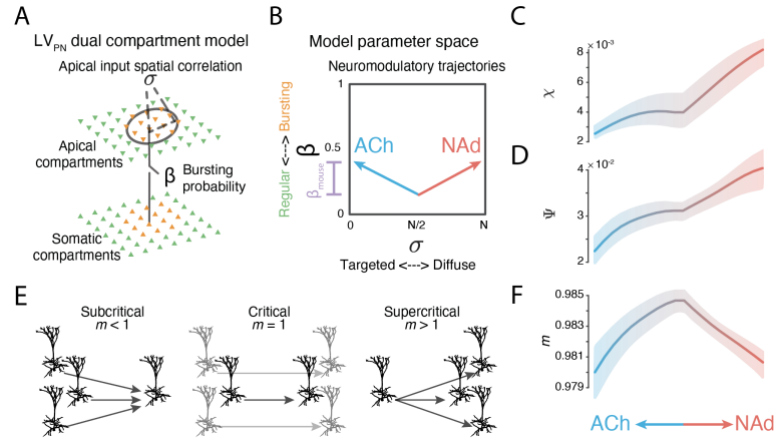


Figure 3 - Biophysically plausible model of nonlinear Layer V pyramidal neurons under neuromodulation recapitulates slightly subcritical dynamics. A) We simulated a neuronal network of LV_{PN} with apical and somatic compartments and isolated the effects of neuromodulation of the cells inherent nonlinearity by changing two parameters: the LV_{PN} burst probability (β) and the apical input spatial correlation (σ). B) Spiking data were simulated across a $[\beta, \sigma]$ model parameter space, within which we could track the hypothetical trajectories of increasing neuromodulatory tone: NAd and ACh both increases bursting probability; however, NAd increases the apical input spatial correlation due to the LC diffuse projections, whereas cholinergic projections are known to be more segregated (Fig. 1A). The neuromodulatory trajectories are constrained within the empirically observed range of mouse Layer V bursting probability (purple bar mean \pm s.d.). C) Temporal spiking variability as quantified by the susceptibility (χ ; thick lines = mean and thin lines = 95th confidence interval) and D) spatial variability as quantified by transient coherence (Ψ ; error-bars are 95th confidence interval) peak following the adrenergic trajectory in parameter space (B) and *v.v.* for cholinergic tone (Measures follow the trajectories outlined in (B)). E) m represents a measure of the proximity of a system to the critical point of a branching process – the panel depicts three typical regimes of a critical branching process: in the subcritical regime (i.e., $m < 1$; left), activity is driven to quiescence; at the critical point (i.e., $m = 1$; middle), activity is self-sustaining; and in the supercritical regime (i.e., $m > 1$; right), activity increases over time. F) Under low neuromodulation, LV_{PN} are near critical, and neuromodulation shifts the system further sub-critical away from the critical point.

cells only burst. Second, we investigated the spatial influence of correlated apical drive, σ (smoothed by a 2-dimensional gaussian with s.d. = σ ; Fig. 3B). This parameter captures differential profiles of apical drive to the system, ranging from bursting LV_{PN} cells that are spatially uncorrelated (i.e., cells are unlikely to be adjacent; $\sigma = 1$) to LV_{PN} cells that are strongly spatially correlated (i.e., cells burst adjacently; $\sigma = N$). We stimulated each parameter combination with identical white noise drive to somatic and apical compartments – before spatial smoothing by σ – and analyzed the emergent spiking dynamics. The combination of nonlinear neurons and diffuse coupling was sufficient to create substantial heterogeneity in the model's emergent spiking dynamics. We also confirmed that an even mixture of spatially correlated bursting and regular spiking was associated with an elevated, albeit low mean pairwise spike-count correlation ($|r_{SC}| < 0.07$), which is consistent with experimental predictions [41].

Based on their differential neuroanatomy, NAd and ACh were hypothesized to have divergent effects on β and σ . Both systems increase β , albeit through different molecular pathways: NAd promotes LV_{PN} bursting via the alpha-2A receptor-mediated closure of HCN-gated I_h channels [27]; and ACh by depolarising M_1 receptors [5]. Despite this similarity, the two systems have divergent effects on σ [2]: adrenergic projections are diffuse and cross-regional boundaries in the cerebral cortex [42], whereas cholinergic projections are typically more segregated [43] (Fig. 1A). For these reasons, in the $[\beta, \sigma]$ model parameter space, the effect of NAd is conceptualized as a right-upward trajectory (red arrows; Fig. 3B), whereas ACh is conceptualized as a left-upward trajectory (blue arrows; Fig. 3B). Note that other mechanisms (not considered here) may move the brain along distinct state-space trajectories, including NMDA receptor engagement, which

increases apical excitability [44] (i.e., an upward trajectory), or non-specific thalamic activity [45], which increases diffuse apical input and excitability (i.e., a right-upward trajectory).

Neuromodulation Shapes Critical Dynamics in Nonlinear Layer V Pyramidal Neurons

To date, theoretical work into criticality within neuronal networks has hypothesized that critical signatures emerge from complex interactions between coalitions of relatively simple (i.e., linear) ‘point’ neurons [7]. This viewpoint has not yet embraced the abundance of inherently nonlinear neurons within the mammalian brain (e.g., LV_{PN} [23,46], whose simple interactions may play a crucial role in the emergence of complex, adaptive dynamics. With our computational model, we can now set the neuromodulatory tone as a constant, enabling us to calculate the proximity to the critical point of the branching process – the universality class of neuronal avalanches [7,33].

We first ensured the model could reproduce our empirical findings (Fig. 2E & F). We found that our model could recapitulate the shifts in spatiotemporal variability of LV_{PN} under both NAd and ACh neuromodulation. Importantly, unlike *in vivo* experiments – which are fundamentally dynamic – we were able to set the model to a constant neuromodulatory tone and hence, calculate both χ and Ψ on the spiking outputs of our model (Fig. 2D) without requiring the dynamic $\hat{\chi}$ and $\hat{\Psi}$ approximation (Fig. 2E & F). Using this approach, we constrained our NAd and ACh trajectories within the empirical bursting regime observed in awake mice (Fig. 3B, purple error-bars). We found evidence to support the hypothesis that NAd and ACh differentially affect the information processing dynamics of the cerebral cortex. Specifically, we demonstrated that NAd increases spatiotemporal variability (Fig. 3C & D, increasing red) by engaging spatially correlated ensembles of bursting LV_{PN}. In contrast, ACh was found to quench spatiotemporal variability (Fig. 3C & D increasing blue) by engaging spatially separated ensembles of bursting LV_{PN} (thin

lines corresponds to 95% confidence intervals across 100 simulations). These modelling results provide robust confirmation of the empirical signatures of the systems-level control of the ascending arousal system on the primary output cell of the cerebral cortex.

Now that we have demonstrated the validity of the nonlinear neuronal model, we can prove the hypothesis that neuromodulation controls critical dynamics in nonlinear LV_{PN}. To do so, we calculated the branching process control parameter, m [9]. The branching process control parameter quantifies one spike’s likelihood to beget a second spike. We calculated this control parameter as,

$$\langle \rho_{t+1} | \rho_t \rangle = m \langle \rho_t \rangle + h, \quad (11)$$

where the population spiking activity in the next time step ρ_{t+1} is determined by the control parameter, m , an external input h , and $\langle . | . \rangle$ is the conditional expectation. m signifies the phase of the system, wherein the critical point ($m = 1$) separates run-away ($m > 1$; supercritical) from quiescent ($m < 1$; subcritical) activity (Fig. 2E). As demonstrated in Fig. 2F, the system is poised close to criticality ($m \sim 0.98$), albeit in a slightly sub-critical, ‘reverberating’ regime [16,33]. A system poised in the reverberating regime can benefit from being near criticality while mitigating its adversary offsets, such as balancing sensitivity vs specificity [47], stimulus detection vs discrimination [48], and integration time, which increases with proximity to the critical point [11].

Unexpectedly, the addition of both NAd and ACh in our model shifts the system into an even more subcritical regime, this is despite both NAd and ACh increasing the bursting likelihood. Interestingly, this finding contradicts the expected result that NAd should shift the system closer to criticality – thereby increasing variability – and vice versa for ACh. Our results indicate that the opposing adaptive modes of NAd and ACh emerge from their respective anatomical projections – the globally controlling diffuse adrenergic neuromodulation promotes variability and flexibility, whereas the locally

controlling targeted cholinergic neuromodulation supports selectivity and reliability. Thus, our finding emphasizes the importance of studying nonlinearities in critical systems, as this phenomenon would not be present in coalitions of linear point-neurons [7]. Our results suggest that the spiking dynamics of LV_{PN} in awake mice are poised near criticality and that neuromodulation can flexibly act as a control parameter shifting the system from this point to utilize the beneficial signatures of criticality while remaining in a neuroprotective slightly subcritical regime.

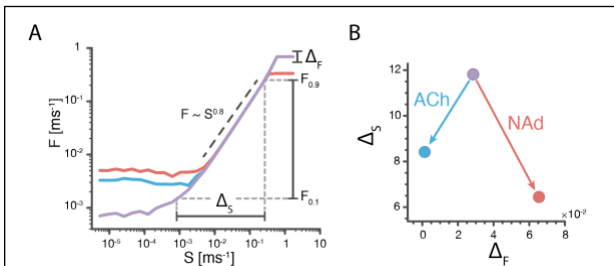


Figure 4 – Functional benefits of critical neuromodulation for information processing.

A) We analysed the information processing of the neural system in the baseline neuromodulatory regime from Fig. 3B (purple) and two regions corresponding to either a cholinergic (blue) or adrenergic (red) phasic burst. The transfer functions between input stimuli intensity S and mean output F across repeated trials, reveals similarities and differences between the three regimes. The dynamic range, Δ_S , and trial-to-trial variability, Δ_F were also calculated. B) the low arousal (purple) had the highest Δ_S (i.e., the highest sensitivity) and moderate Δ_F , whereas ACh (blue) minimised Δ_F and thus increases specificity and signal reliability, whereas NAAd (red) maximised Δ_F and hence promoted a more flexible information processing mode.

Critical Dynamics Mediate Functional Information Processing Modes

Based on these results, we further hypothesized that cholinergic and adrenergic neuromodulation should differentially augment the network's receptivity to incoming stimuli [2]: NAAd should augment flexibility and variability (albeit nonlinearly) [3], whereas ACh should enhance reliability and selectivity [49], analogous to widening or focusing

the width of the flashlight, respectively. A robust method for probing a system's information processing capacity is to investigate its transfer function (or input-output/gain curve), which maps a precise input to a characteristic output. In psychophysics, a typical transfer function fit to experimental data is the power-law function $F(S) \sim S^\alpha$, known as Stevens law, where S is the stimulus intensity, α the scaling 'Stevens' exponent, and $F(S)$ is the neural response to the stimulus [50]. An efficient transfer function possesses an $\alpha < 1$ as this allows a given range of stimuli to be mapped onto a smaller output range. We calculated the transfer function as,

$$F(S) = \frac{1}{T} \sum_{t=1}^T \rho_t(S), \quad (12)$$

which is the mean spike density response, $F(S)$, to afferent Poisson spikes, ρ_t , with a mean-rate S randomly distributed across the network. A useful metric that can be calculated from the transfer function are the dynamic-range,

$$\Delta_S = 10 \log_{10} \left(\frac{S_{0.9}}{S_{0.1}} \right), \quad (13)$$

which represents the range of discriminable stimuli [12]. The range $[S_{0.1}, S_{0.9}]$ are inverted from the transfer function $[F_{0.1}, F_{0.9}]$ with $F_x = F_0 + x(F_\infty - F_0)$ where F_∞ and F_0 represent the saturation and baseline response, respectively. Another useful measure is the trial-to-trial variability of the transfer function,

$$\Delta_F = \langle \text{Var}(10 \log_{10} F(S)) \rangle, \quad (14)$$

representing the intrinsic reliability and variability in mapping a stimulus to output [47].

To test our hypothesis, we calculated the transfer function in three regions of parameter space, which were chosen to represent the awake state (i.e., the base of the neuromodulatory trajectories in Fig. 3B; Fig. 4A purple; $\sigma = 39$, $\beta = 0.2$), as well as under

either adrenergic (Fig. 3B tip red arrow; Fig. 4A red; $\sigma = 52.3, \beta = 0.44$) or cholinergic (Fig. 3B tip blue arrow; Fig. 4A blue; $\sigma = 25.7, \beta = 0.44$) neuromodulation. We found the three transfer functions all followed a power-law between their baseline and saturation values with the same scaling exponent $\alpha \sim 0.8$, suggesting they efficiently map a large stimuli range to a smaller output, and that the psychophysical-law is invariant to arousal state (i.e., equivalent differences in stimulus lead to a proportional change in perceived magnitude across arousal). (Fig. 4A). It should be emphasized that these properties are emergent phenomena and have not been coded into the network. The low neuromodulation regime (purple) possessed the largest dynamic range, Δ_S , (Fig. 4B), consistent with its proximity to the critical point (Fig. 3F). Increasing NAd led to the largest trial-to-trial variability, Δ_F , (Fig. 4B; red), which is consistent with the theory that NAd facilitates flexible behaviour (i.e., a diffuse flashlight beam; 2). In contrast, increasing ACh led to a reduction in variability (Fig. 4B blue), corresponding to an increase in stimuli specificity and reliability, consistent with the known enhancement of stimulus detectability and focus with the increased cholinergic tone, i.e., a focused flashlight beam [49].

Our findings thus present an optimal solution to the inefficiency of subcritical dynamics and pitfalls of near-critical dynamics [47]: the unaroused (low neuromodulatory) brain is associated with optimal signal detection (sensitivity), and two highly-conserved neuromodulatory axes either sharpen specificity and reliability (ACh) or widen the flexibility of the system (NAd).

Discussion

Our results demonstrated a biological implementation for controlling different information processing modes in the brain – namely, by using distinct arms of the ascending arousal system as control parameters to mediate population-level, slightly subcritical dynamics in nonlinear cortical neurons. We found adrenergic and cholinergic

modulation could adaptively facilitate flexible and reliable information processing modes and somewhat unexpectedly shifted the network into a neuro-protective slightly subcritical regime demonstrated by a branching parameter less than unity. Nevertheless, despite this subcritical shift away from the critical point, the interaction between adrenergic and cholinergic anatomical projections and LV_{PN} apical dendrites led to opposing beneficial adaptive dynamics – increasing and decreasing χ and Ψ , respectively, which are typically prescribed to a one-dimensional critical phase transition [21–24]. In this way, our results thus provide a natural resolution to the fundamental problem attributed to the critical brain hypothesis: namely, that while criticality is beneficial for information processing [9,13,14,16,51,52], being poised near criticality is biologically risky, as it can lead to runaway activity (such as seizures) [10].

Through our findings, we can re-interpret canonical results from experimental neuroscience. For instance, the association of ACh with a heightened focus [53] may relate to its capacity to constrain the variability of spatiotemporal neural dynamics. Similarly, the relationship between NAd tone and both cognitive function [3] and adaptability [54] can be reframed as arising from the augmentation of inherent nonlinearities within populations of pyramidal cells within the cerebral cortex. Furthermore, this result provides insight into the large variability in trial-to-trial responses to identical stimuli observed in animal recordings [55]. The slow-drift in response variability likely corresponds to fluctuations in neuromodulatory tone, changing the system's neural gain. In particular, experiments have demonstrated quenched variability at the onset of stimulus trials [56], which in our model corresponds to an increase in cholinergic tone. We predict that other arms of the ascending arousal system, such as the dopaminergic, serotonergic, and histaminergic systems (to name a few), will play similar roles as control parameters, albeit constrained by the unique circuits that these systems innervate.

In conclusion, the confusion surrounding how biological neuromodulation can mediate beneficial information processing dynamics without pushing the system too close to the supercritical phase in the awake, mammalian brain can be rationalized by incorporating their anatomical and physiological properties. Whereby, despite both adrenergic and cholinergic neuromodulation increasing the bursting likelihood and shifting the system into a more subcritical regime – due to their differential anatomical intersection with the apical dendrites of LV_{PN} – they can adaptively mediate distinct signatures of criticality. Specifically, diffuse adrenergic projections promoted spatiotemporal neuronal variability, whereas targeted cholinergic projections quenched spatiotemporal neuronal variability. We demonstrated that a dual – local vs global – control of dynamics is an effective technique for efficient neural operation emphasized as the brain processes many critical biological functions, such as conscious perception and feedforward-feedback integration, through neuromodulatory altered LV_{PN} . Thus, understanding how neuromodulation alters LV_{PN} neuronal dynamics is essential for the effective treatment of pathologies in cognitive function caused by failures of the neuromodulatory system, such as dementia, and incorporating this dual-controllability into other dynamical learning systems, such as neural network organization, will likely be beneficial.

Acknowledgments

We would like to thank Matthew Larkum, Michael Breakspear, Russell A. Poldrack, Cristopher Whyte, Rick Shine, and Paul Martin for their constructive notes on the manuscript. The Harris Lab and Janelia for their public repository of Eight-probe Neuropixels recordings in three mice. JMS was supported by an NHMRC Investigator grant (#1193857) and a University of Sydney Robinson Fellowship.

References:

- [1] J. M. Shine, E. J. Müller, B. Munn, J. Cabral, R. J. Moran, and M. Breakspear, *Computational Models Link Cellular Mechanisms of Neuromodulation to Large-Scale Neural Dynamics*, Nat Neurosci (2021).
- [2] J. M. Shine, *Neuromodulatory Influences on Integration and Segregation in the Brain*, Trends in Cognitive Sciences **23**, 572 (2019).
- [3] G. Aston-Jones and J. D. Cohen, *An Integrative Theory of Locus Coeruleus-Norepinephrine Function: Adaptive Gain and Optimal Performance*, Annu. Rev. Neurosci. **28**, 403 (2005).
- [4] T. W. Schmitz and J. Duncan, *Normalization and the Cholinergic Microcircuit: A Unified Basis for Attention*, Trends in Cognitive Sciences **22**, 422 (2018).
- [5] S. R. Williams and L. N. Fletcher, *A Dendritic Substrate for the Cholinergic Control of Neocortical Output Neurons*, Neuron **101**, 486 (2019).
- [6] M. Suzuki and M. E. Larkum, *General Anesthesia Decouples Cortical Pyramidal Neurons*, Cell **180**, 666 (2020).
- [7] J. M. Beggs and D. Plenz, *Neuronal Avalanches in Neocortical Circuits*, J. Neurosci. **23**, 11167 (2003).
- [8] G. Tkačik, T. Mora, O. Marre, D. Amodei, S. E. Palmer, M. J. Berry, and W. Bialek, *Thermodynamics and Signatures of Criticality in a Network of Neurons*, Proc Natl Acad Sci USA **112**, 11508 (2015).
- [9] M. A. Muñoz, *Colloquium: Criticality and Dynamical Scaling in Living Systems*, Rev. Mod. Phys. **90**, 031001 (2018).
- [10] L. Cocchi, L. L. Gollo, A. Zalesky, and M. Breakspear, *Criticality in the Brain: A Synthesis of Neurobiology, Models and Cognition*, Progress in Neurobiology **158**, 132 (2017).
- [11] E. J. Müller, B. Munn, and J. M. Shine, *Diffuse Neural Coupling Mediates Complex Network Dynamics through the Formation of Quasi-Critical Brain States*, Nat Commun (2020).
- [12] O. Kinouchi and M. Copelli, *Optimal Dynamical Range of Excitable Networks at Criticality*, Nature Phys **2**, 348 (2006).
- [13] W. L. Shew and D. Plenz, *The Functional Benefits of Criticality in the Cortex*, Neuroscientist **19**, 88 (2013).
- [14] B. R. Munn, *Critical Spatiotemporal Dynamics of the Brain’s Endogenous Activity and Its Natural Stimuli*, University of Sydney, 2019.
- [15] H. Hinrichsen, *Nonequilibrium Critical Phenomena and Phase Transitions into Absorbing States*, Advances in Physics **49**, 815 (2000).
- [16] J. Wilting and V. Priesemann, *Between Perfectly Critical and Fully Irregular: A Reverberating Model Captures and Predicts Cortical Spike Propagation*, Cerebral Cortex **29**, 2759 (2019).
- [17] N. Friedman, S. Ito, B. A. W. Brinkman, M. Shimono, R. E. L. DeVille, K. A. Dahmen, J. M. Beggs, and T. C. Butler, *Universal Critical Dynamics in High Resolution Neuronal Avalanche Data*, Phys. Rev. Lett. **108**, 208102 (2012).
- [18] B. Munn, E. J. Müller, G. Wainstein, and J. M. Shine, *The Ascending Arousal System Shapes Low-Dimensional Brain Dynamics to Mediate Awareness of Changes in Intrinsic Cognitive States*, preprint, Neuroscience, 2021.
- [19] J. M. Shine, *The Thalamus Integrates the Macrosystems of the Brain to Facilitate Complex, Adaptive Brain Network Dynamics*, Progress in Neurobiology **199**, 101951 (2021).
- [20] R. V. Williams-García, M. Moore, J. M. Beggs, and G. Ortiz, *Quasicritical Brain Dynamics on a Nonequilibrium Widom Line*, Phys. Rev. E **90**, 062714 (2014).
- [21] J. Aru, M. Suzuki, R. Rutiku, M. E. Larkum, and T. Bachmann, *Coupling the State and Contents of Consciousness*, Front. Syst. Neurosci. **13**, 43 (2019).
- [22] N. Takahashi, T. G. Oertner, P. Hegemann, and M. E. Larkum, *Active Cortical Dendrites Modulate Perception*, Science **354**, 1587 (2016).
- [23] M. Larkum, *A Cellular Mechanism for Cortical Associations: An Organizing*

- Principle for the Cerebral Cortex*, Trends in Neurosciences **36**, 141 (2013).
- [24] M. E. Larkum, J. J. Zhu, and B. Sakmann, *A New Cellular Mechanism for Coupling Inputs Arriving at Different Cortical Layers*, Nature **398**, 338 (1999).
- [25] S. R. Williams, *Dependence of EPSP Efficacy on Synapse Location in Neocortical Pyramidal Neurons*, Science **295**, 1907 (2002).
- [26] M. L. S. Tantirigama, T. Zolnik, B. Judkewitz, M. E. Larkum, and R. N. S. Sachdev, *Perspective on the Multiple Pathways to Changing Brain States*, Front. Syst. Neurosci. **14**, 23 (2020).
- [27] C. Labarrera, Y. Deitcher, A. Dudai, B. Weiner, A. Kaduri Amichai, N. Zylbermann, and M. London, *Adrenergic Modulation Regulates the Dendritic Excitability of Layer 5 Pyramidal Neurons In Vivo*, Cell Reports **23**, 1034 (2018).
- [28] C. Stringer, M. Pachitariu, N. Steinmetz, C. B. Reddy, M. Carandini, and K. D. Harris, *Spontaneous Behaviors Drive Multidimensional, Brainwide Activity*, Science **364**, eaav7893 (2019).
- [29] J. J. Jun, N. A. Steinmetz, J. H. Siegle, D. J. Denman, M. Bauza, B. Barbarits, A. K. Lee, C. A. Anastassiou, A. Andrei, Ç. Aydın, M. Barbic, T. J. Blanche, V. Bonin, J. Couto, B. Dutta, S. L. Gratiy, D. A. Gutnisky, M. Häusser, B. Karsh, P. Ledochowitsch, C. M. Lopez, C. Mitelut, S. Musa, M. Okun, M. Pachitariu, J. Putzeys, P. D. Rich, C. Rossant, W. Sun, K. Svoboda, M. Carandini, K. D. Harris, C. Koch, J. O’Keefe, and T. D. Harris, *Fully Integrated Silicon Probes for High-Density Recording of Neural Activity*, Nature **551**, 232 (2017).
- [30] Q. Wang, S.-L. Ding, Y. Li, J. Royall, D. Feng, P. Lesnar, N. Graddis, M. Naeemi, B. Facer, A. Ho, T. Dolbeare, B. Blanchard, N. Dee, W. Wakeman, K. E. Hirokawa, A. Szafer, S. M. Sunkin, S. W. Oh, A. Bernard, J. W. Phillips, M. Hawrylycz, C. Koch, H. Zeng, J. A. Harris, and L. Ng, *The Allen Mouse Brain Common Coordinate Framework: A 3D Reference Atlas*, Cell **181**, 936 (2020).
- [31] J. Reimer, M. J. McGinley, Y. Liu, C. Rodenkirch, Q. Wang, D. A. McCormick, and A. S. Tolias, *Pupil Fluctuations Track Rapid Changes in Adrenergic and Cholinergic Activity in Cortex*, Nat Commun **7**, 13289 (2016).
- [32] Z. Mridha, J. W. de Gee, Y. Shi, R. Alkashgari, J. Williams, A. Suminski, M. P. Ward, W. Zhang, and M. J. McGinley, *Graded Recruitment of Pupil-Linked Neuromodulation by Parametric Stimulation of the Vagus Nerve*, Nat Commun **12**, 1539 (2021).
- [33] J. Wilting and V. Priesemann, *Inferring Collective Dynamical States from Widely Unobserved Systems*, Nat Commun **9**, 2325 (2018).
- [34] W. Gerstner, A. K. Kreiter, H. Markram, and A. V. M. Herz, *Neural Codes: Firing Rates and Beyond*, Proceedings of the National Academy of Sciences **94**, 12740 (1997).
- [35] M. Girardi-Schappo, G. S. Bortolotto, J. J. Gonsalves, L. T. Pinto, and M. H. R. Tragtenberg, *Griffiths Phase and Long-Range Correlations in a Biologically Motivated Visual Cortex Model*, Sci Rep **6**, 29561 (2016).
- [36] H. Yang, W. L. Shew, R. Roy, and D. Plenz, *Maximal Variability of Phase Synchrony in Cortical Networks with Neuronal Avalanches*, Journal of Neuroscience **32**, 1061 (2012).
- [37] E. M. Izhikevich, *Simple Model of Spiking Neurons*, IEEE Transactions on Neural Networks **14**, 1569 (2003).
- [38] M. E. Larkum, *Top-down Dendritic Input Increases the Gain of Layer 5 Pyramidal Neurons*, Cerebral Cortex **14**, 1059 (2004).
- [39] B. W. Connors and M. J. Gutnick, *Intrinsic Firing Patterns of Diverse Neocortical Neurons*, Trends in Neurosciences **13**, 99 (1990).
- [40] S. Heitmann, T. Boonstra, and M. Breakspear, *A Dendritic Mechanism for Decoding Traveling Waves: Principles and Applications to Motor Cortex*, PLoS Comput Biol **9**, e1003260 (2013).
- [41] A. Renart, J. de la Rocha, P. Bartho, L. Hollender, N. Parga, A. Reyes, and K. D.

- Harris, *The Asynchronous State in Cortical Circuits*, Science **327**, 587 (2010).
- [42] E. Samuels and E. Szabadi, *Functional Neuroanatomy of the Noradrenergic Locus Coeruleus: Its Roles in the Regulation of Arousal and Autonomic Function Part II: Physiological and Pharmacological Manipulations and Pathological Alterations of Locus Coeruleus Activity in Humans*, CN **6**, 254 (2008).
- [43] L. Zaborszky, L. Hoemke, H. Mohlberg, A. Schleicher, K. Amunts, and K. Zilles, *Stereotaxic Probabilistic Maps of the Magnocellular Cell Groups in Human Basal Forebrain*, NeuroImage **42**, 1127 (2008).
- [44] M. E. Larkum, T. Nevian, M. Sandler, A. Polsky, and J. Schiller, *Synaptic Integration in Tuft Dendrites of Layer 5 Pyramidal Neurons: A New Unifying Principle*, Science **325**, 756 (2009).
- [45] M. J. Redinbaugh, J. M. Phillips, N. A. Kambi, S. Mohanta, S. Andryk, G. L. Dooley, M. Afrasiabi, A. Raz, and Y. B. Saalman, *Thalamus Modulates Consciousness via Layer-Specific Control of Cortex*, Neuron S0896627320300052 (2020).
- [46] M. Häusser and B. Mel, *Dendrites: Bug or Feature?*, Current Opinion in Neurobiology **13**, 372 (2003).
- [47] L. L. Gollo, *Coexistence of Critical Sensitivity and Subcritical Specificity Can Yield Optimal Population Coding*, J. R. Soc. Interface **14**, 20170207 (2017).
- [48] W. P. Clawson, N. C. Wright, R. Wessel, and W. L. Shew, *Adaptation towards Scale-Free Dynamics Improves Cortical Stimulus Discrimination at the Cost of Reduced Detection*, PLoS Comput Biol **13**, e1005574 (2017).
- [49] M. E. Hasselmo, *The Role of Acetylcholine in Learning and Memory*, Current Opinion in Neurobiology **16**, 710 (2006).
- [50] A. Reina, T. Bose, V. Trianni, and J. A. R. Marshall, *Psychophysical Laws and the Superorganism*, Sci Rep **8**, 4387 (2018).
- [51] L. Barnett, J. T. Lizier, M. Harré, A. K. Seth, and T. Bossomaier, *Information Flow in a Kinetic Ising Model Peaks in the Disordered Phase*, Phys. Rev. Lett. **111**, 177203 (2013).
- [52] J. M. Beggs and N. Timme, *Being Critical of Criticality in the Brain*, Front. Physiol. **3**, (2012).
- [53] M. E. Hasselmo and J. McGaughy, *High Acetylcholine Levels Set Circuit Dynamics for Attention and Encoding and Low Acetylcholine Levels Set Dynamics for Consolidation*, in *Progress in Brain Research*, Vol. 145 (Elsevier, 2004), pp. 207–231.
- [54] S. Bouret and S. J. Sara, *Network Reset: A Simplified Overarching Theory of Locus Coeruleus Noradrenaline Function*, Trends in Neurosciences **28**, 574 (2005).
- [55] A. S. Ecker, P. Berens, R. J. Cotton, M. Subramaniyan, G. H. Denfield, C. R. Cadwell, S. M. Smirnakis, M. Bethge, and A. S. Tolias, *State Dependence of Noise Correlations in Macaque Primary Visual Cortex*, Neuron **82**, 235 (2014).
- [56] M. M. Churchland, B. M. Yu, J. P. Cunningham, L. P. Sugrue, M. R. Cohen, G. S. Corrado, W. T. Newsome, A. M. Clark, P. Hosseini, B. B. Scott, D. C. Bradley, M. A. Smith, A. Kohn, J. A. Movshon, K. M. Armstrong, T. Moore, S. W. Chang, L. H. Snyder, S. G. Lisberger, N. J. Priebe, I. M. Finn, D. Ferster, S. I. Ryu, G. Santhanam, M. Sahani, and K. V. Shenoy, *Stimulus Onset Quenches Neural Variability: A Widespread Cortical Phenomenon*, Nat Neurosci **13**, 369 (2010).
- [57] Q. Wang, W. W. S. Yue, Z. Jiang, T. Xue, S. H. Kang, D. E. Bergles, K. Mikoshiba, S. Offermanns, and K.-W. Yau, *Synergistic Signaling by Light and Acetylcholine in Mouse Iris Sphincter Muscle*, Current Biology **27**, 1791 (2017).
- [58] J. Szentágothai, *The ‘Module-Concept’ in Cerebral Cortex Architecture*, Brain Research **95**, 475 (1975).